

PROCESSING OF PLANE STRAIN COMPRESSION TEST RESULTS FOR INVESTIGATION OF AISI-304 STAINLESS STEEL CONSTITUTIVE BEHAVIOR

Sergey A. Aksenov¹, Jiri Kliber², Yuriy A. Puzino¹, Stanislav A. Bober¹

¹ National Research University,
Higher School of Economics,
Department of Applied Mathematics,
Tallinskaya 34, 123458, Moscow, Russia
E-mail: saksenov@hse.ru

Received 15 February 2015
Accepted 01 September 2015

² VŠB - Technical University of Ostrava,
17. listopadu 15, 708 33, Ostrava - Poruba,
Czech Republic

ABSTRACT

The paper is oriented toward the determination of constitutive equation constants by the inverse analysis of plane strain compression test results. The interpretation of such results is complicated by the inhomogeneity of strain rate distribution in the specimen caused by rigid ends, the lateral spreading of a specimen friction and the variation of temperature during the test. The results of plane strain compression tests of AISI-304 stainless steel are presented and significant deviations of temperature are observed at higher strain rates. Finite element simulation was performed to estimate the inhomogeneity of strain rate within the specimen and evaluate the effect of friction on the test results. Constitutive equations of the material were obtained by inverse analysis minimizing the deviations between the measured load values and the ones predicted by numerical simulation.

Keywords: PSCT, AISI-304, Gleeble, constitutive equations, hot forming, FEM, inverse analysis.

INTRODUCTION

Specification of constitutive equations describing the material flow stress is necessary for the design and optimization of technological procedures in forming [1]. Computer aided simulation of forming processes based on the finite element method is applied in the optimization of energy consumptions of production, preventing defects in the product, reducing the load on the equipment, increasing the utilization of a material and solving other technological tasks [2 - 7]. The accuracy of constitutive models used in such simulations is critical.

Various tests are used in the evaluation of material constitutive behavior: uniaxial and biaxial tensile tests, blow forming tests, torsion tests and compression tests (ring compression, plane strain compression). The type of a test should generally correspond to the stress strain mode realized in the simulated forming process. The plane strain compression test (PSCT) is generally adopted for studies of a material flow behavior during

flat rolling [8] due to the fact that the stress-strain mode corresponding to flat rolling is very similar to the ideal plane strain compression.

Interpretation of PSCT results is complicated by inhomogeneity of strain rate in the volume of the specimen caused by rigid ends, variance of specimen temperature, friction between the specimen and the tools and lateral spreading of the specimen. The inhomogeneity of strain rate distribution and lateral spreading of the specimen are responsible for the fact that stress-strain data obtained from PSCT depends on the geometry of a specimen and tools. At the same time, the flow stress is a material property and should not depend on the geometrical characteristics of the specimen. Thus, the corrections of stress-strain data obtained from PSCT should be made to obtain real constitutive equations of the material. Different techniques were developed for the correction of PSCT data [8 - 14]. The inverse analysis appears to be a most powerful of them providing the way of determining constitutive equation constants [12 - 14] or

evaluating microstructure models [15]. The objective of this work is the application of the inverse analysis to the characterization of AISI-304 stainless steel constitutive behavior in a wide range of temperatures and strain rates.

EXPERIMENTAL

AISI-304 stainless steel samples of standard chemical composition were tested at constant nominal temperature of 1000°C in nominal strain rate range of 0.01 - 10 s⁻¹ and at constant nominal strain rate of 1 s⁻¹ in the temperature range of 800 - 1100°C. Prior to deformation the specimens were heated to a temperature of 1200°C, held one minute and cooled to the temperature of deformation. The initial specimen geometry was a brick of 20 mm wide, 15 mm long and 10 mm thick. The specimens were deformed by the tool of 5 mm thick to the nominal strain of 1. Graphite lubricants and tantalum foils were used in order to eliminate friction between specimens and the tools. The temperature was measured by a thermocouple placed in the middle of the lateral surface of the specimen. The experiments were performed on Gleeble 3800 testing machine.

The data obtained during the tests were reordered to a protocol containing the following information: current time, measured load, measured specimen temperature, measured displacement of the tool, nominal displacement of the tool, nominal temperature, calculated value of the effective strain, calculated value of the effective stress. Thus, only four parameters are measured during the test: time, load, displacement and temperature. Effective strain and strain rate are calculated according to the following formulas [8]:

$$\varepsilon = \frac{2}{\sqrt{3}} \ln \left(\frac{h_0 + 2\delta}{h_0} \right) \quad (1)$$

$$\sigma = \frac{\sqrt{3} F}{2 S_0} \quad (2)$$

where h_0 is the initial thickness of the specimen, S_0 is the initial square of the contact between the specimen and δ is the tool, is the tool displacement, F is the measured load.

RESULTS AND DISCUSSION

Approximation of data stress-strain

Based on the ideas expressed in [16 - 21], the ap-

proximation of constitutive behavior of steel in conditions of hot forming can be constructed as a set of equations taking into account strain hardening, dynamic recovery and dynamic recrystallization processes:

$$\sigma = X_d \sigma_{drx} + (1 - X_d) \sigma_{drv} (1 - \exp(-\Omega \varepsilon))^m \quad (3)$$

$$X_d = 1 - \exp(-k(\varepsilon - \varepsilon_c))^n \quad (4)$$

$$\varepsilon_c = A_e \left(\dot{\varepsilon} \cdot \exp \left(\frac{Q_e}{RT} \right) \right)^d \quad (5)$$

$$\sigma_{drx} = \frac{1}{\alpha_{drx}} \operatorname{asinh} \left(A_{drx} \left(\dot{\varepsilon} \cdot \exp \left(\frac{Q_{drx}}{RT} \right) \right)^{m_x} \right) \quad (6)$$

$$\sigma_{drv} = \frac{1}{\alpha_{drv}} \operatorname{asinh} \left(A_{drv} \left(\dot{\varepsilon} \cdot \exp \left(\frac{Q_{drv}}{RT} \right) \right)^{m_v} \right) \quad (7)$$

where: X_d is treated as a dynamically recrystallized fraction; ε_c - critical strain for initialization of dynamic recrystallization; $R(=8.31)$ is the universal gas constant; $\Omega, m, k, n, A_e, Q_e, d, \alpha_{drx}, \alpha_{drv}, A_{drx}, A_{drv}, m_x, m_v, Q_{drx}$ and Q_{drv} are the constants to be determined.

The experimental stress-strain data were approximated by eq. (3 - 7) using the least square method and the Nelder-Mead [22] minimization procedure. The results of approximation compared with Gleeble data are presented in Fig. 1 and Fig. 2.

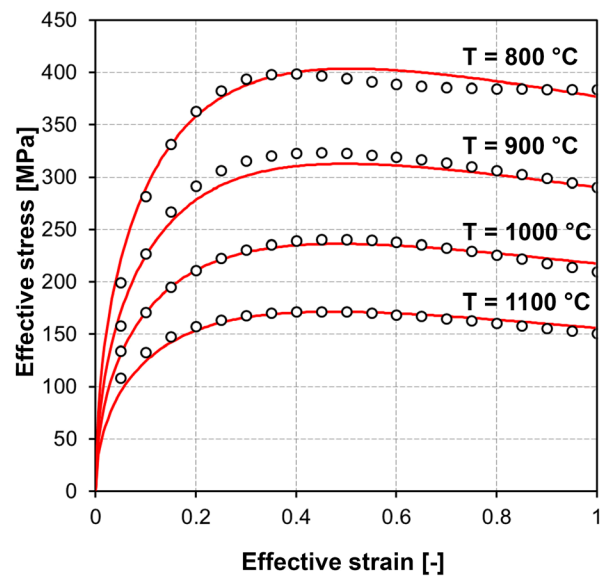


Fig. 1. Stress-strain curves obtained by PSCT at strain rate of 1 s⁻¹.

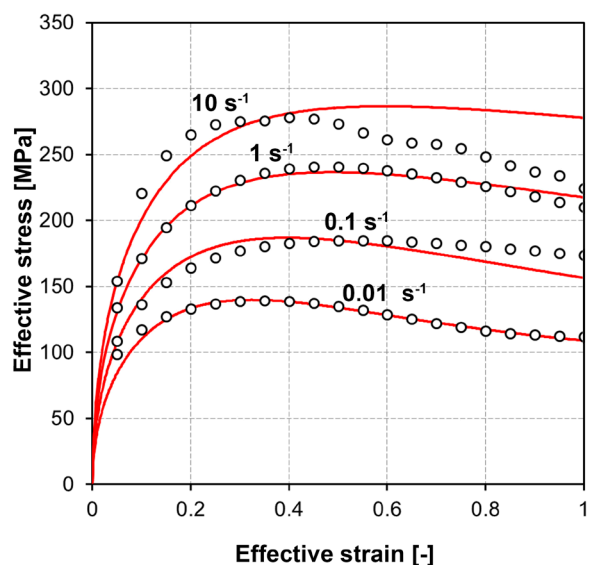


Fig. 2. Stress-strain curves obtained by PSCT at temperature of 1000°C.

The approximation fits all the stress-strain curves obtained experimentally except the one corresponding to the strain rate 10 s^{-1} and the temperature of 1000°C. The reason of such deviation is that in this case the nominal experimental conditions were not satisfied correctly as it can be seen from the proper analysis of the experimental data. Fig. 3 illustrates the measured temperature of the specimen. The actual strain-rate calculated by numerical derivation of strain is plotted in Fig. 4 versus nominal strain. It can be clearly seen that the temperature is not constant and it rises by approximately 20°C during the test. At the same time, the strain rate varies in about a 30 % range when the strain is less than 0.7 and then decreases to the value of 6 s^{-1} . The strain rate variation in the rest of experiments was less than 1 %.

Temperature variations observed in the tests performed at the nominal strain rate of 1 s^{-1} are presented in Fig. 5. It can be seen that the temperature varies in a range of about 15°C during the tests at this strain rate. These variations should be taken into account during the processing of PSCT data. Temperature variations during the tests at lower strain rates are in the negligible range of 1°C.

As the constitutive equations specified above are constructed by the approximation of data obtained directly from Gleeble protocol they need to be corrected. Stress-strain data collected in the protocol are calculated according to the equations (1) and (2), which does not take into account the flow in homogeneities caused by

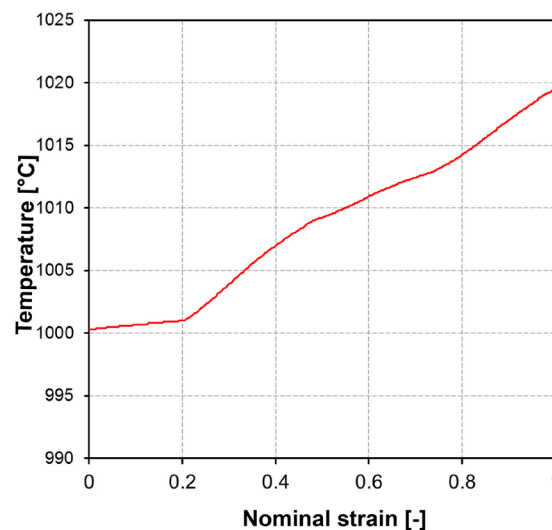


Fig. 3. Temperature variation during the test at temperature of 1000°C and nominal strain rate of 10 s^{-1} .

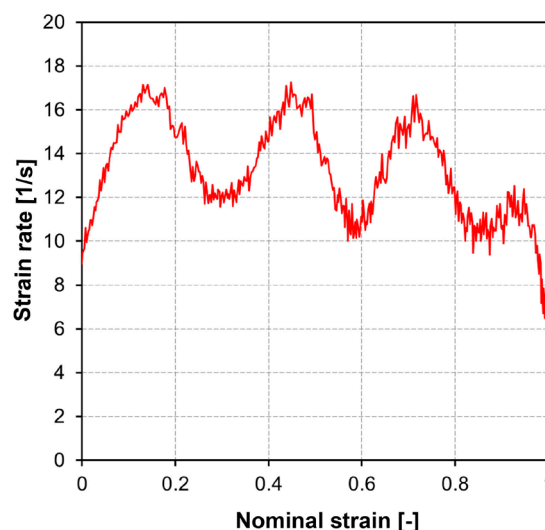


Fig. 4. Actual strain rate variation during the test at temperature of 1000°C and nominal strain rate of 10 s^{-1} .

the rigid ends, lateral spreading and temperature variation taking place during the test. Thus the approximation obtained is used only as an initial guess for the inverse analysis based on FE simulation.

Finite element simulation

The aim of finite element simulation of PSCT is to predict the evolution of force acting on tools as much correctly as possible. Comparison between the measured forces and the predicted ones allows one to estimate an

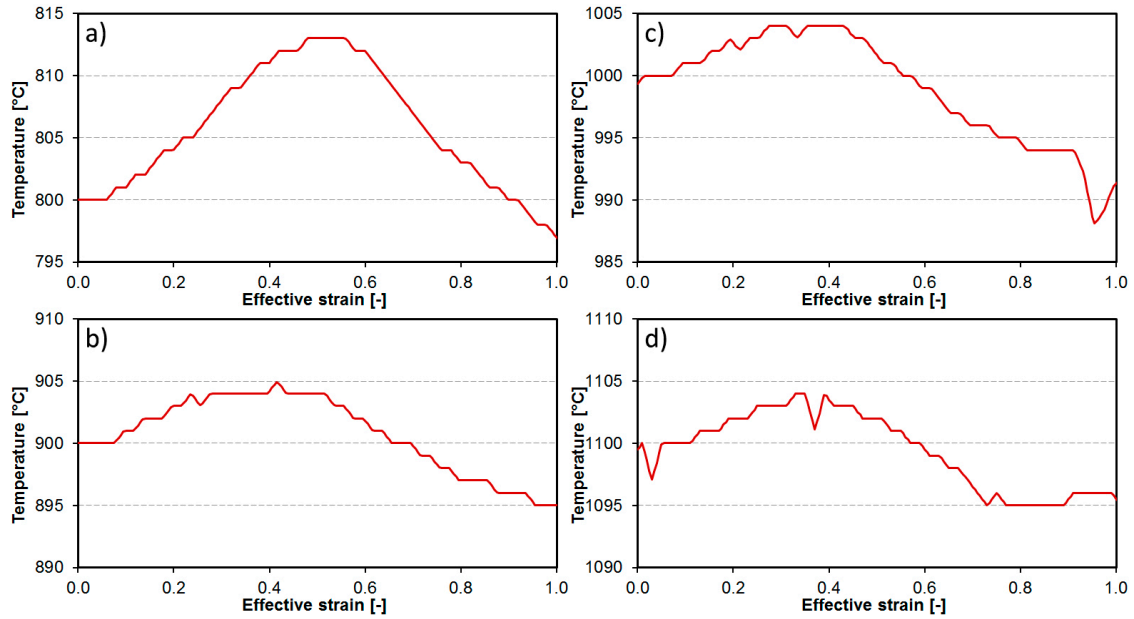


Fig. 5. Temperature variations of the tests at nominal strain rate of 1 s^{-1} and different nominal temperatures: a) 800°C ; b) 900°C ; c) 1000°C ; d) 1100°C .

adequacy of constitutive equations used for simulation. The constitutive equation constants then should be iteratively corrected to minimize the deviations between the measured values and the predicted ones. 3D FE simulation produces more accurate results but it is also time consuming for use in the inverse analysis. At the same time, the conditions of metal flow during PSCT are very close to ideal plane strain deformation so 2D FE simulation could be efficiently used.

Loads predicted by 2D FE simulation are generally lower at large strains than ones obtained by solving a full 3D task because of the lateral spreading which is neglected in 2D models. Applying the corrections proposed in [10] the actual value of load can be estimated as:

$$F = \frac{F_{2D} b}{b_0 (C_1 \exp(\delta/C_2) + C_3)} \quad (8)$$

where F_{2D} is the load obtained by 2D FE simulation, δ is the current toll displacement, C_1 , C_2 and C_3 are the empirical constants ($C_1 = 0.048$, $C_2 = 1.37 \text{ mm}$, $C_3 = 1.04$ [10]), b_0 is the initial breadth of the specimen and b is the actual one. Actual specimen width b can be calculated using the formulas proposed in [13]:

$$b = b_0 \left(1 + C - C \left(\frac{h}{h_0} \right)^{0.18} \right) \quad (9)$$

$$C = \frac{b_f/b_0 - 1}{1 - (h_f/h_0)^{0.18}} \quad (10)$$

where b_f is the final width, h_0 is the initial height and h_f is the final height of the specimen.

In order to estimate the influence of friction between the specimen and the tool on the evolution of load during PSCT a series of simulations with different friction factor values was performed. The comparison of load vs. nominal strain curves obtained for different friction factors is presented in Fig. 6. It can be seen that friction does not play a significant role until the nominal strain is less than 1.

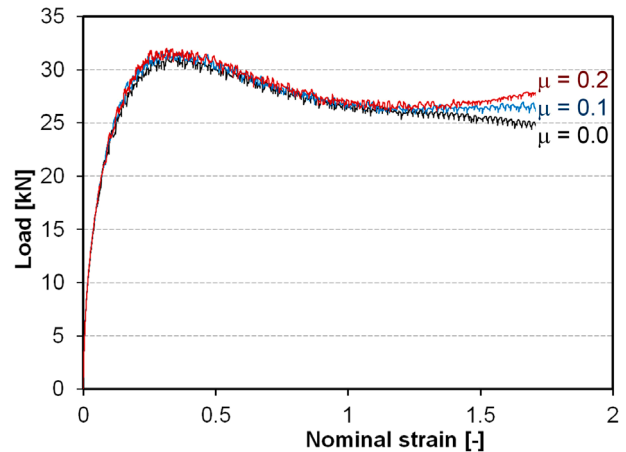


Fig. 6. Evolution of the load calculated for different friction factors.

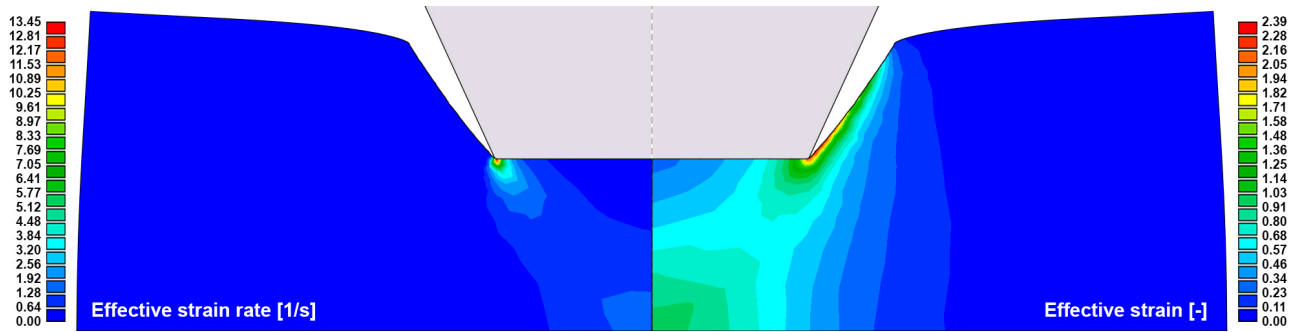


Fig. 7. Geometry of cross section and the distributions of strain and strain rate corresponding to nominal strain of 0.6 obtained by FE simulation of PSCT at temperature of 800°C and strain rate of 1 s⁻¹.

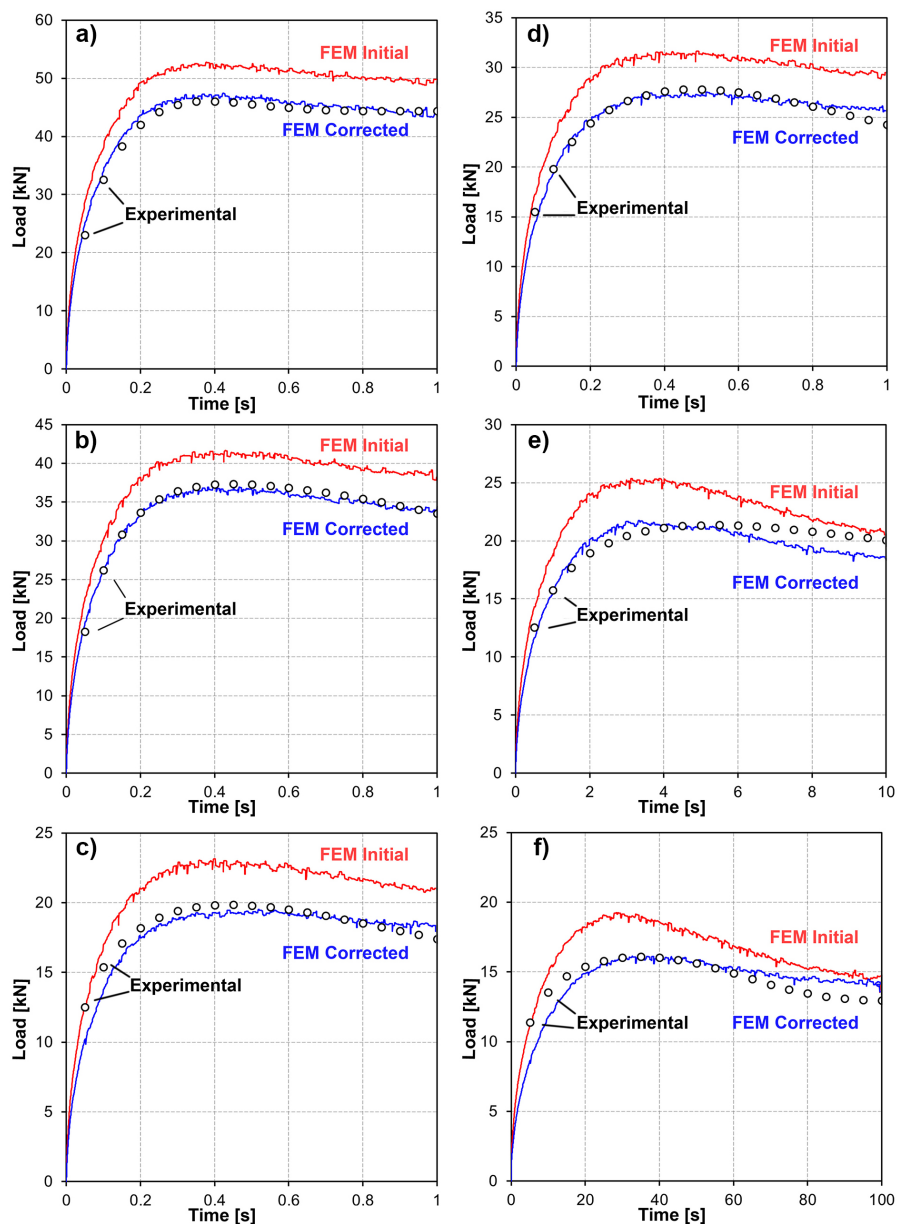


Fig. 8. The comparison of the experimental loads with predicted ones obtained before and after the correction of constitutive equations for temperatures and strain rates of: a) 800°C, 1 s⁻¹; b) 900°C, 1 s⁻¹; c) 1100°C, 1 s⁻¹; d) 1000°C, 1 s⁻¹; e) 1000°C, 0.1 s⁻¹; f) 1000°C, 0.01 s⁻¹.

Finite element simulation of PSC tests was performed using 2D three-node triangle elements. The friction factor value used for the simulations is 0.15. The temperature was considered to be distributed uniformly in a specimen volume and vary with time according to the measured values. Due to the symmetry of the task it was reduced to consideration of one quarter of specimen section. Distributions of the effective strain and effective strain rate obtained by simulation are presented in Fig. 7.

Correction of constitutive equations

The comparison of predicted loads with the experimental ones is presented in Fig. 8. It can be seen that before the correction of constitutive equations, the loads obtained by FEM are 10 - 20 % higher than the experimental ones. The initial values of constitutive equation constants were corrected to minimize the objective function:

$$E = \sum_{i=1}^N \frac{1}{t_i} \int_0^{t_i} (F_m(t) - F(t))^2 dt \quad (11)$$

where N is the number of tests, t_i is the duration of the i -th test, F_m is the measured load and F is the load predicted by FEM.

Fig. 8 represents the load evolution obtained by FE simulation after the correction of constitutive equation constants. The values of the constants before and after correction are listed in Table 1.

CONCLUSIONS

The stress-strain data obtained by the plane strain compression test should be corrected to produce reliable data for constitutive equations. Temperature variations could be taken into account by using the measured values instead of the nominal ones in FE simulation solving a direct problem during the inverse analysis. Friction does not affect significantly the evolution of load during PSCT of samples with the initial geometry of 10x15x20 (mm) until the nominal strain is less than 1.

A series of PSC tests of AISI-304 stainless steel was performed for the temperature range of 800 - 1100°C and the nominal strain rates in the range of 0.01 - 10 s⁻¹. Large temperature variations were observed during the tests at higher strain rates. The constitutive model describing the material behavior was constructed using

Table 1. The values of constitutive equation constants before and after the correction.

Constant	Initial approximation	Corrected value
Ω	6.05	6.01
m	0.49	0.49
k	0.0187	0.0187
n	1.59	1.6
A_e	0.1094	0.1099
Q_e	3050	15328
d	0.2113	0.214
$1/\alpha_{drx}$	17.05	8.466
$1/\alpha_{drv}$	36.431	36.5
A_{drx}	8.34E-12	1.09E-11
A_{drv}	3.29E-9	3.25E-9
m_x	0.3522	0.3746
m_v	0.5298	0.5277
Q_{drx}	966000	1084000
Q_{drv}	514000	500000

the inverse analysis of PSCT data taking into account the temperature variations and the effective strain-rate inhomogeneity occurring during the tests.

Acknowledgements

The study was implemented in the framework of the Basic Research Program at the National Research University Higher School of Economics (HSE) in 2015.

REFERENCES

1. R. Fabik, J. Kliber, I. Mamuzic, T. Kubina, S.A. Aksenov, Mathematical modelling of flat and long hot rolling based on finite element methods (FEM), *Metalurgija*, 51, 3, 2012, 341-344.
2. S.K. Choi, M.S. Chun, C.J. Van Tyne, Y.H. Moon, Optimization of open die forging of round shapes using FEM analysis, *Journal of Materials Processing Technology*, 172,1, 2006, 88-95.
3. H. Grass, C. Krempaszky, E. Werner, 3-D FEM-simulation of hot forming processes for the production of a connecting rod, *Computational Materials Science*, 36, 4, 2006, 480-489.
4. E.N. Chumachenko, I.V. Logashina, S.A. Aksenov, Simulation modeling of rolling in passes, *Metallurgist*, 50, 7-8, 2006, 413-418.
5. L. Giorleo, E. Ceretti, C. Giardini, Energy consumption reduction in Ring Rolling processes: A FEM analysis, *International Journal of Mechanical Sciences*, 74, 2013, 55-64.

6. T.I. Cherkashina, I.P. Mazur, S.A. Aksenov, Soft reduction of a cast ingot on the incomplete crystallization stage, *Materials Science Forum*, 762, 2013, 261-265.
7. I.P. Mazur, Improvement of consumer properties and stability of the technological process of hot rod stock production, *Materials Science Forum*, 575-578, 2008, 379-384.
8. A.J. Lacey, M.S. Loveday, G.J. Mahon, B. Roebuck, C.M. Sellars, M.R. van der Widen, Measuring flow stress in hot plane strain compression tests, *Mater. High Temp.*, 23, 2, 2006, 85-118.
9. N.J. Silk, M.R. van der Widen, Interpretation of hot plane strain compression testing of aluminium specimens, *Material Science and Technology*, 5, 1999, 295300.
10. B. Kowalski, C.M. Sellars, M. Pietrzyk, Identification of rheological parameters on the basis of plane strain compression test on specimens of various initial dimensions, *Computational Materials Science*, 35, 2006, 9297.
11. J.C. Gelin, O. Ghossein, M. Pietrzyk, An inverse method for determining viscoplastic properties of aluminium alloys, *Journal of Materials and Technology*, 45, 1994, 435440.
12. D. Szeliga, E. Gawad, M. Pietrzyk, Inverse analysis for identification of rheological and friction models in metal forming, *Computer methods in applied mechanics and engineering*, 195, 2006, 67786798.
13. B. Kowalski, W. Wajda, M. Pietrzyk, C.M. Sellars, Influence of strain and strain rate inhomogeneity on constitutive equations determined from plane strain compression tests, *Proceedings of 4th ESAFORM Conference on Materials Forming*, University of Liege, 2001, 561564.
14. D. Szeliga, P. Matuszyk, R. Kuziak, M. Pietrzyk, Identification of rheological parameters on the basis of various types of plasometric tests, *Journal of Materials Processing Technology*, 125-126, 2002, 150154.
15. J. Kliber, S. Aksenov, R. Fabík, Numerical study of deformation characteristics in plane strain compression test (PSCT) volume certified following microstructure, *Metalurgija*, 48, 4, 2009, 257-261.
16. Y. Liu, W. Shi, Experimental Study on Constitutive Equation of AZ31 Magnesium Alloy Plastic Deformation at Elevated Temperature, *Transactions of International Conference on Physical and Numerical Simulation*, 2007.
17. R. Kuziak, Y. Chen, M. Głowacki, M. Pietrzyk, Modeling of the microstructure and mechanical properties of steel during thermomechanical processing, *Technical Note 1393*, November 1997, 80.
18. M.A. Shafaat, H. Omidvar, B. Fallah, Prediction of hot compression flow curves of Ti-6Al-4V alloy in α - β phase region, *Materials & Design*, 32, 10, 2011, 4689-4695.
19. D. Feng, X.M. Zhang, S.D. Liu, Y.L. Deng, Constitutive equation and hot deformation behavior of homogenized Al-7.68Zn-2.12Mg-1.98Cu-0.12Zr alloy during compression at elevated temperature, *Materials Science and Engineering: A*, 608, 2014, 63-72.
20. R. Fabík, T. Kubina, S. Aksenov, K. Drozd, I. Schindler, J. Kliber, Verification of new model for calculation of critical strain for the initialization of dynamic recrystallization using laboratory rolling, *Metalurgija*, 48, 4, 2009, 273-276.
21. G. Quan, G. Luo, J. Liang, D. Wu, A. Mao, Q. Liu, Modelling for the dynamic recrystallization evolution of Ti-6Al-4V alloy in two-phase temperature range and a wide strain rate range, *Computational Materials Science*, 97, 2015, 136-147.
22. J.A. Nelder, R. Mead, A simplex method for function minimization, *Computer Journal*, 7, 1965, 308-313.